Journal of Mathematical Biology (2022) 85:46
https://doi.org/10.1007/s00285-022-01813-4

Mathematical Biology

A cancer model with nonlocal free boundary dynamics

Avner Friedman[1] · Wenrui Hao[2] · King-Yeung Lam[3]

Received: 7 September 2021 / Revised: 8 September 2022 / Accepted: 17 September 2022 /
Published online: 7 October 2022

Abstract
Cancer cells at the tumor boundary move in the direction of the oxygen gradient, while cancer cells far within the tumor are in a necrotic state. This paper introduces a simple mathematical model that accounts for these facts. The model consists of cancer cells, cytotoxic T cells, and oxygen satisfying a system of partial differential equations. Some of the model parameters represent the effect of anti-cancer drugs. The tumor boundary is a free boundary whose dynamics is determined by the movement of cancer cells at the boundary. The model is simulated for radially symmetric and axially symmetric tumors, and it is shown that the tumor may increase or decrease in size, depending on the "strength" of the drugs. Existence theorems are proved, global in-time in the radially symmetric case, and local in-time for any shape of tumor. In the radially symmetric case, it is proved, under different conditions, that the tumor may shrink monotonically, or expand monotonically.

Keywords Free boundary problem · Cancer modeling · Solution existence · Treatment studies

Mathematics Subject Classification 35R35 · 35Q92 · 35A35

1 Introduction

We consider a tumor region $\Omega(t)$ in 3-D space with boundary $\partial\Omega(t)$ that varies in time. Within $\Omega(t)$ there are cancer cells with density $C(x,t)$ and other species with densities/concentrations $X_i(x,t)$ $(1 \le i \le m)$. These variables satisfy a system of partial differential equations (PDEs) of the following form:

B Wenrui Hao
wxh64@psu.edu

1 Mathematical Biosciences Institute & Department of Mathematics, The Ohio State University, Columbus, OH 43210, USA

2 Department of Mathematics, The Pennsylvania State University, University Park, PA 16802, USA

3 Department of Mathematics, The Ohio State University, Columbus, OH 43210, USA

$$\frac{\partial C}{\partial t} - \delta_C \nabla^2 C = \lambda_C(X) C\left(1 - \frac{C}{K}\right) - F(X)C, \tag{1.1}$$

$$\frac{\partial X_i}{\partial t} - \delta_{X_i} \nabla^2 X_i = \lambda_{X_i}(X, C) - d_{X_i}(X, C) X_i \quad (1 \le i \le m), \tag{1.2}$$

where $X = (X_1, \ldots, X_m)$, δ_C and δ_{X_i} are diffusion coefficients, λ_C and λ_{X_i} are growing rates of C and X_i, F and d_{X_i} are killing rate of C and death/degradation rates of X_i, and K is the carrying capacity of cancer cells. The species X_i are cells, proteins or other molecules.

The variables C and X_i satisfy boundary conditions on $\partial(t)$, but the boundary is unknown, it is a free boundary that needs to be determined together with the solution of the PDE system. A fundamental question is how to derive the law that governs the dynamics of the free boundary $\partial(t)$.

This question was addressed by Byrne and Chaplain (1997), starting with the assumption that

$$C(x, t) \equiv \text{const. for all } x \in \Omega(t), \ t \ge 0. \tag{1.3}$$

They introduced variables σ (externally-supplied nutrients), β (externally-supplied inhibitors), and ω (internally-produced inhibitors) satisfying diffusion equations

$$\nabla^2 \sigma + F_\sigma = \nabla^2 \beta + F_\beta = \nabla^2 \omega + F_\omega = 0 \text{ in } \Omega(t)$$

with appropriate boundary conditions on $\partial(t)$, and a proliferation rate func-tion $S(\sigma, \beta, \omega)$. Assuming that cancer cells move with velocity $\vec{v}(x, t)$, and taking $C(x, t) \equiv 1$, the mass conservation law yields the equation

$$\nabla \cdot \vec{v}(x, t) = S(\sigma, \beta, \omega)(x, t). \tag{1.4}$$

Byrne and Chaplain (1997) specify the dynamics of the free boundary $\Omega(t)$ by defining, for each $(x, t) \in \partial(t)$, the velocity in the outward normal direction, $n(x, t)$, as

$$V_n(x, t) = \vec{v}(x, t) \cdot n(x, t). \tag{1.5}$$

Eq. (1.5) alone does not, of course, define the vector $\vec{v}(x, t)$, except in the case where the tumor and all variables are radially symmetric. In the non-radially symmetric case, another condition is needed, such as Darcy's law

$$\vec{v} = -\nabla p,$$

where p is the pressure within cancer cells in $\Omega(t)$, or Stokes equation which relates μ to ∇p by a PDE system.

The assumption (1.3) was extended to the general systems (1.1 and 1.2) with cells $X_1, \ldots, X_k$, and proteins and molecules $X_{k+1}, \ldots, X_m$, by taking

$$C(x,t) + \sum_{i=1}^{k} X_i(x,t) \equiv \text{ const. for all } x \in \Omega(t),\ t \geq 0;$$

see review in (Friedman 2018, Chapter 6). This condition was used also in other free boundary problems that arise in biology, for example in the growth of plaques in atherosclerosis (Friedman and Hao 2015; Hao and Friedman 2014) and in multiple sclerosis (Moise and Friedman 2020) and in the growth of granuloma in tuberculosis (Hao et al. 2016) and in leishmaniasis (Siewe et al. 2017).

Motivated by the fact that the density of cancer cells is definitely far from being constant throughout the tumor (see for instance Dini et al. 2016; Freyer and Sutherland 1986; Gallaher et al. 2019), we develop in this paper an alternative approach to defining the velocity of the free boundary. We denote the volume of $\Omega(t)$ by $V(t)$ and note that the growth of $V(t)$ is positively correlated to the growth of the total mass of cancer cells in $\Omega(t)$, so that

$$\frac{dV(t)}{dt} = \mu(t,C) \int_{\Omega(t)} \frac{\partial C(x,t)}{\partial t}\,dx, \tag{1.6}$$

where $\mu(t,C)$ is a positively-valued function that depends on t and the aggressiveness of the cancer. In Sect. 2 we explain how to use the system (1.1 and 1.2) and boundary conditions to determine the relation between the movement of $\partial\Omega(t)$ and $\frac{dV(t)}{dt}$, and this, in conjunction with Eq. (1.6), will provide the nonlocal dynamics of the free boundary in terms of $\mu(t,C)$.

For clarity, we shall do this for a simple PDE system that includes just C and two other species, namely, effector T cells (T) and oxygen (w).

In Sect. 2, we develop the mathematical model; the model includes several parameters which represent the effect of anti-cancer drugs. Simulations of the model, under different drug treatments, are given in Sect. 3 in the case of radially symmetric tumors, and, in Sect. 4, in the case of axially symmetric tumors. In Sect. 5, we prove the existence of solutions of radially symmetric tumors, for all $t > 0$, andin Sect. 6 we prove local-in-time existence for the case of general shaped tumors. Section 7 is concerned with the behavior of the free boundary $r = R(t)$ of radially symmetric tumors. Taking the killing rate of cancer cells by T cells as a parameter η, we prove that for η large, $dR(t)/dt < 0$, while, for η small, $dR(t)/dt > 0$, and the tumor can grow to any size if η is arbitrarily decreased.

2 Mathematical model

The function $\mu(t, C)$ in Eq. (1.6) may depend on the specific cancer and on the shape of the tumor. For simplicity we take it to be just a positive function of t, $\mu(t)$, so that

$$\frac{dV(t)}{dt} = \mu(t) \int_{(t)} \frac{\partial C(x,t)}{\partial t} dx \quad \text{for } t > 0. \tag{2.1}$$

The concentration of oxygen, $w(x, t)$, within the tumor decreases from the tumor rim toward the tumor core. Hence, the tumor proliferation rate also decreases from the rim toward the core. We account for this situation by taking the proliferation rate of C to be $\lambda_C \frac{[w-w_h]^+}{w_0-w_h}$ where w_0 is the concentration of oxygen in healthy tissue and w_h is an hypoxic level below which cancer cells do not proliferate; they are either in senescence or, if they died, their debris remains in the tumor. Naturally, we have $w_0 > w_h$.

In addition to oxygen $w(x, t)$, we introduce in the model also cytotoxic T cells ($CD8^+$ T cells), $T(x, t)$, which kill cancer cells at some constant rate η. Hence the equation for C takes the following form:

$$\frac{\partial C}{\partial t} - \delta_C \nabla^2 C = \lambda_C \frac{[w - w_h]^+}{w_0 - w_h} C\left(1 - \frac{C}{K}\right) - \eta T C \text{ in } (t), \text{ for } t > 0. \tag{2.2}$$

Dendritic cells, a professional antigen-presenting cells that link innate and adaptive immunity, recognize cancer cells, and then activate the T cells. Noting that T cells use primarily anaerobic respiration to support bioenergetic needs (Salmond 2018; van der Windt and Pearce 2012), we denote the proliferation rate of T by $\lambda_T C$ for some parameter λ_T, independent of w. Denoting by d_T the death rate of T cells, the equation for T cells then takes the following form:

$$\frac{\partial T}{\partial t} - \delta_T \nabla^2 T = \lambda_T C - d_T T \text{ in } (t), \text{ for } t > 0.$$

We shall consider an anti-cancer treatment which increases tumor immunogenicity (ITI) (Wu and Waxman 2018), that is, it increases the ability of cancer to induce immune response that can prevent its growth. We represent the effect of this treatment by an increase in the parameter λ_T.

We shall also consider anti-cancer treatment by immune checkpoint blockade. T cells have receptors, such as PD-1, that serve as checkpoints, while cancer cells express the ligands PD-L1. The complex PD-1/PD-L1 deactivates T cells. A drug that inhibits PD-1, increases the anti-cancer activity of T cells (Postow et al. 2015; Li et al. 2018; Fares et al. 2019). We represent the effect of such a drug by an increase in the parameter η.

We shall finally consider cancer vaccines that serve to enlarge the pool of tumor-specific T cells which are dormant in the lymph nodes (van der Burg et al. 2016). GVAX is a common cancer vaccine composed of tumor cells genetically modified to secrete GM-CSF and then irradiated to prevent further cell division. GM-CSF can

activate dendritic cells (Kaufman et al. 2014; Gupta and Emens 2010; Simmons et al. 2007) which then activate dormant T cells. We represent the effect of the vaccine by adding a source $\varepsilon d_T T_0$ to the T-equation, where T_0 is the density of the inactive (naive or dormant) T cells from the lymph nodes, so that

$$\frac{\partial T}{\partial t} - \delta_T \nabla^2 T = \lambda_T C - d_T(T - \varepsilon T_0) \text{ in } \Omega(t), \text{ for } t > 0; \tag{2.3}$$

since, in steady state with $C \equiv 0$, T should be no greater than T_0, the parameter ε is restricted to the interval $0 \le \varepsilon d_T \le 1$.

We assume that oxygen is consumed at constant rate by cancer cells, so that

$$\frac{\partial w}{\partial t} - \delta_w \nabla^2 w = -d_{wC} C w - d_w w \text{ in } \Omega(t), \text{ for } t > 0, \tag{2.4}$$

where d_{wC} and d_w are constants.

Since there are no cancer cells outside $\Omega(t)$, C satisfies a boundary condition of the from

$$\alpha \frac{\partial C}{\partial n} + (1 - \alpha) C = 0 \text{ on } \partial\Omega(t), \text{ for } t > 0,$$

for some $0 \le \alpha \le 1$, where $n(x, t)$ is the outward normal to $\partial\Omega(t)$ at x. We take $\alpha = 1$ so that

$$\frac{\partial C}{\partial n} = 0 \text{ on } \partial\Omega(t), \text{ for } t > 0, \tag{2.5}$$

but all the analysis and simulation results of this paper can be extended to the case where $0 < \alpha < 1$. Since $C > 0$ on the tumor rim, the case $\alpha = 0$ can be excluded.

We assume that

$$\frac{\partial T}{\partial n} + \gamma(t)(T - T_0) = 0 \text{ on } \partial\Omega(t), \text{ for } t > 0,$$
$$\text{where } \gamma(t) > 0 \text{ if } T < T_0, \ \gamma(t) = 0 \text{ if } T \ge T_0. \tag{2.6}$$

Cancer cells under hypoxia secrete vascular endothelial growth factor (VEGF) that induces the formation of new blood capillaries around the tumor, resulting in increased oxygen concentration at the boundary $\partial\Omega(t)$ to some level W above w_0; W can be decreased by treatment with VEGF inhibitor, a commonly used drug. We take

$$w = W \text{ on } \partial\Omega(t), \text{ for } t > 0, \text{ where } W \ge w_0, \tag{2.7}$$

assuming that $W = w_0$ under effective treatment with VEGF inhibitor.

We next consider the dynamics of the free boundary. We assume that cancer cells that are on the boundary at time $t = 0$ remain on the boundary for all $t > 0$; more precisely, that the movement of boundary points coincides with the movement of cancer

cells at these boundary points. We consider first the case where $\sigma(t)$ is increasing for $0 \le t \le t_0$.

Cancer cells proliferate abnormally fast, and require increased supply of oxygen. We assume that cancer cells at a point $x = x(t) \in \partial\Omega(t)$ move in the direction of the gradient $\nabla w(x,t)$ (of increased oxygen concentration) with velocity proportional to $|\nabla w(x,t)|$, so that

$$\frac{dx(t)}{dt} = \rho(t)\nabla w(x(t),t) \text{ in } \Omega(t),\ t > 0; \tag{2.8}$$

hence the movement of $x(t)$ along the outward normal $n(x(t),t)$ is given by

$$\frac{dx(t)}{dt}\cdot n(x,t) = \rho(t)\frac{\partial w(x(t),t)}{\partial n(x,t)} \text{ on } \partial\Omega(t),\ t > 0, \tag{2.9}$$

where the function $\rho(t)$ is to be determined.

During a small time interval $(t, t+\Delta t)$, the boundary points of $\partial\Omega(t)$ span a region of volume approximated by

$$V(t+\Delta t) - V(t) \approx \rho(t)\frac{\partial w(x(t),t)}{\partial n(x,t)}\,dS_x\cdot\Delta t,\ \partial\Omega(t)$$

where dS_x is the area element on $\partial\Omega(t)$. Taking Δt arbitrarily small, we get

$$\frac{dV(t)}{dt} = \rho(t)\ \partial\Omega(t)\ \frac{\partial w(x(t),t)}{\partial n(x,t)}\,dS^x.$$

Substituting $\frac{dV}{dt}$ from Eq. (2.1) with $\frac{\partial C}{\partial t}$ from Eq. (2.2), and using the non-flux boundary condition (2.5), we find that

$$\rho(t) = \frac{\mu(t)\quad \lambda\ [w-w_h]^+ C\,1 - \frac{C}{} - \eta TC\,dx}{(t)\quad C\frac{}{w_0-w_h}\ \partial\Omega(t)\ \frac{\partial w(x(t),t)}{\partial n(x,t)}\,dS_x^K}. \tag{2.10}$$

Since we assumed that $\Omega(t)$ is increasing for $0 \le t \le t_0$, we expect $\rho(t)$ to be positive for $0 \le t \le t_0$. If $\rho(t) < 0$ for $0 \le t \le t_0$ (for example when ηT is large), it means that the $\Omega(t)$ is actually decreasing. In this case we assume that the T cells push back the points x on $\partial\Omega(t)$ in the reverse direction of $\nabla w(x,t)$ with a velocity proportional to $|\nabla w(x,t)|$, and we find, as before, that the proportionality coefficient is $\rho(t)$ given by the same equation (2.10). Thus, regardless of whether $\Omega(t)$ is increasing or decreasing, the dynamics of the free boundary is given by the system (2.8, 2.9 and 2.10).

To summarize: the surfaces $\partial\Omega(t)$, $t > 0$, are spanned by the points whose velocity is given by Eq. (2.8), and, in the normal direction, by Eq. (2.9), where $\rho(t)$ is defined by Eq. (2.10), and (w, C, T) is the solution of the PDE system (2.2, 2.3, 2.4, 2.5, 2.6 and 2.7) in

$$^{t} = \{(x, \tau) : x \in (\tau) \text{ and } 0 \le \tau \le t\}$$

with prescribed initial conditions.

In the special case where (t), C, T and w are radially symmetric, we have

$$(t) = \{0 \le r \le R(t)\}, \ \partial(t) = \{r = R(t)\}, \tag{2.11}$$

and $C = C(r, t)$, $T = T(r, t)$, $w = w(r, t)$ where $r = |x|$, and

$$\frac{dR(t)}{dt} = \rho(t)\frac{\partial w(R(t), t)}{\partial r} = \frac{3\mu(t)}{R(t)^2}\int_0^{R(t)} \lambda_C \frac{[w - w_h]^+}{w_0 - w_h} C\left(1 - \frac{C}{K}\right) - \eta T C\, r^2\, dr. \tag{2.12}$$

Parameter values used in the model simulations are given in Table 1.

3 Numerical results for radially symmetric tumors

The choice of $\mu(t)$ determines how fast the tumor volume grows. In the numerical simulations, for radially symmetric tumors, we take

$$\mu(t) = 2 + t/5, \ \gamma(t) = \begin{cases} 1 & \text{if } T \le T_0, \\ 0 & \text{if } T > T_0, \end{cases}$$

and the following initial conditions:

$$d = 0.1 \text{ cm}, \quad R(0) = 0.5 \text{ cm}, \quad C(r, 0) = 0.9K\frac{([r - R(0) + d]^+)^2}{d^2},$$
$$w(r, 0) = (W - w_h)\frac{([r - R(0) + d]^+)^2}{d^2},$$
$$T(r, 0) = T_0 \min\left(\frac{([r - R(0) + 2d]^+)^2}{d^2}, 1\right).$$

In the following three figures, we consider the case where the tumor was already treated with VEGF inhibitor, so that $W = w_0$.

Figure 1 with $\eta = 100$, $\lambda_T = 4 \times 10^{-3}$ shows the average density of C, T and w over 180 days, and the corresponding growth of the tumor radius from $R(0) = 0.5$ to $R(180) = 1.8$ cm. We see that as the tumor radius increases, the average density of oxygen is decreasing, while the average densities of C and T are increasing in the first 50 days and then remain almost constant. We also see that, at $t = 180$ days, the spatial densities of C, T, and w are increasing from the tumor center $r = 0$ to the tumor boundary $r = R(180)$. We note, in particular, that the necrotic core, where $w < w_h$, is approximately the region $0 \le r < 0.7$ cm, and in this region there are hardly any T cells; T cells are mostly present where the cancer cells are proliferating, and their density correlates to the density of cancer cells.

Table 1 Parameter description and value: Est = estimated and TW = this work

Parameter	Description	Value
δ_C	Diffusion coefficient of cancer cells	8.64×10^{-7} cm^2 day^{-1} (Lai and Friedman 2019)
δ_T	Diffusion coefficient of T-cell	8.64×10^{-7} cm^2 day^{-1} (Lai and Friedman 2019)
δ_w	Diffusion coefficient of oxygen	2 cm^2 day^{-1} (Friedman and Siewe 2020)
w_0	Concentration of oxygen in healthy tissue	4×10^{-6} g/cm^{-3} (Friedman and Siewe 2020)
w_h	Hypoxic level of oxygen	2.5×10^{-6} g/cm^{-3} (Friedman and Siewe 2020)
d_T	Death rate of T cells	0.18/day (Lai and Friedman 2019)
d_w	Consumption rate of oxygen	1.04/day (Lai and Friedman 2019)
d_{wC}	Consumption rate of oxygen by cancer cells	2.08/day TW
λ_C	Proliferation rate of cancer cells	2.24 day^{-1} (Lai and Friedman 2019)
λ_T	Cancer-induced proliferation rate of T cells	4×10^{-3} day^{-1} (Lai and Friedman 2019) & Est
T_0	Level of naive T cells	10^{-3} g/cm^{-3} (Lai and Friedman 2019) & Est
K	Carrying capacity of cancer cells	0.4(Lai and Friedman 2019)

Figure 1 with $\eta = 100$ and $\lambda_T = 4 \times 10^{-2}$, an increase of the parameter λ_T by a factor of 10, represents a treatment by ITI therapy. Tumor radius was substantially decreased, and, in particular, $R(180) = 1.4$ cm compared to 1.8 cm without ITI therapy. As a result, the average oxygen concentration is much higher and, in particular, it is above the hypoxic level w_h by day 180.

Treatment by anti-PD-1 means an increase in the effective killing rate η of cancer cells by T cells. Fig. 1 with $\eta = 500$ and $\lambda_T = 4 \times 10^{-3}$ shows that such treatment reduced $R(180)$ from 1.8 cm to 0.9 cm, the oxygen concentration has increased and the necrotic core decreased, from $0 \le r < 0.5$ to $0 \le r < 0.2$ cm.

In Fig. 2 we simulated the effect of treatment with cancer vaccine ($\varepsilon = 2$) and gradually increasing anti-PD-1 (η). Starting with $R(0) = 0.5$ cm, we see that the radius growth decreases as η increases. In the case where $\lambda_T = 4 \times 10^{-3}$, $\eta = 500$, the radius $R(180) = 1.3$ cm in Fig. 1, when $\varepsilon = 0$, is significantly reduced to $R(180) = 0.7$ cm with vaccine treatment at $\varepsilon = 2$. We also see an initial oscillation in $R(t)$ and in the cancer average density $C(t)$. Such oscillations were observed also in Friedman et al. (2006) and can be explained as follows: If $C(t)$ decreases then $\lambda_T C$, and hence T decreases, so the killing rate ηT of C decreases and this may result in an increase in C soon after time t.

4 3D numerical results for axially symmetric tumors

In this section, we consider axially symmetric tumor, that is, all species are functions of (r, z) where $r = \sqrt{x^2 + y^2}$, and

$$\Omega(t) = \{(r, z); |z| \le R(r, t)\}.$$

To simulate $\Omega(t), t > 0$, we discretize the spatial direction by using the finite difference method, solve the semi-discretized temporal system by using the explicit Runge-Kutta 4th order scheme. In particular, we use the uniform grid points on the ϑ direction with a stepsize $\vartheta = \frac{2\pi}{m}$, namely, $\vartheta_j = j\vartheta$, $j = 0, \ldots, m-1$ where m is the number of grid points. For the radius on each ϑ_j direction, we use the uniform grid points with a stepsize h_j, namely, $r_{i,j} = \rho_j + i h_j$ with $h_j = \frac{R - \rho_j}{n}$ and $i = 0, 1, \ldots, n$, where n is the number of grid points on each radius. Then we use the central difference scheme to approximate the derivatives for both r and ϑ.

Figure 3 shows 2 rows of tumors with $\mu(t) = 2 + t$ and $\lambda_T = 4 \times 10^{-3}$. In the first row, $\eta = 1000$ and $\varepsilon = 0$ and in the second row, $\eta = 10000$ and $\varepsilon = 0.1$. In the first row, tumor volume increases in time, and in the second row, the tumor volume is decreasing.

If the oxygen concentration is linearly decreasing along the internal normal to the boundary, then, as tumor volume increases, boundary points near a reentrant corner should be moving with greater velocity than points away from the reentrant corner, and this results in a decrease in the reentrant corner. Indeed, this is clearly seen in the two simulations of the top row in Fig. 3. Conversely, for the same reason, as tumor volume decreases, boundary points near reentrant corner recede further than boundary points elsewhere, as seen in the second simulation of the bottom row in Fig. 3. Fingers, as in

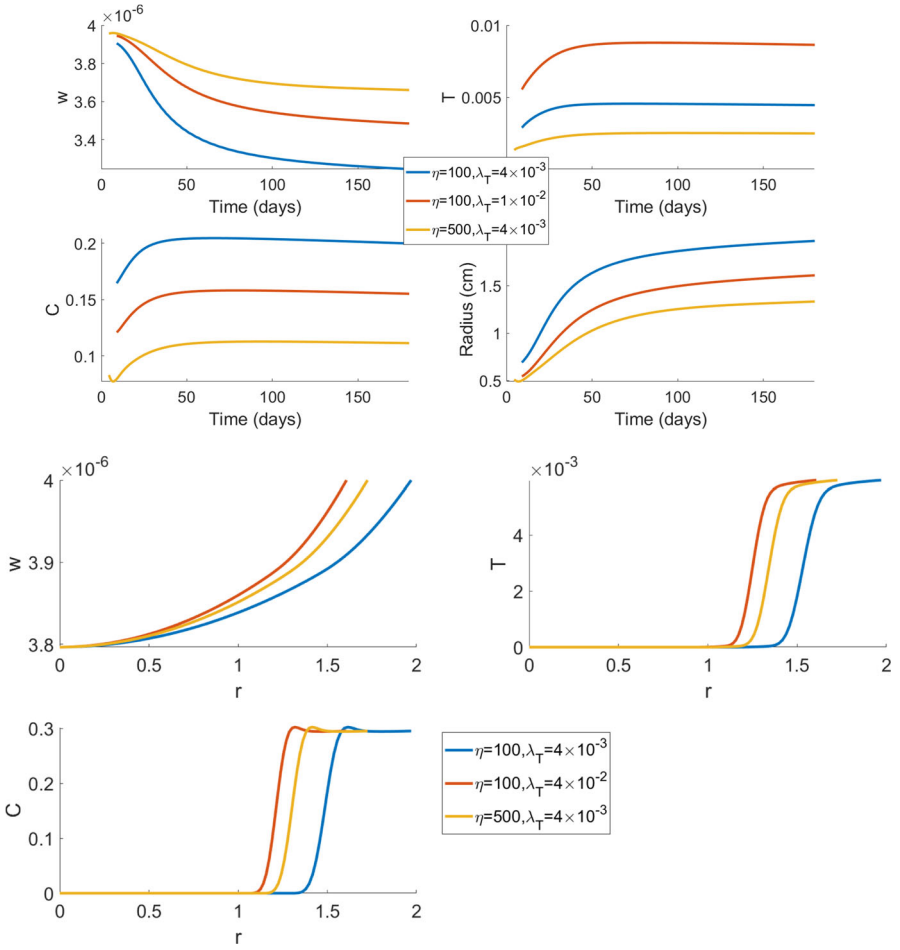

Fig. 1 Treatment with VEGF inhibitor. $W = w_0$ on the free boundary, with $\varepsilon = 0$ and different λ_T and η. The first four figures describe the dynamic of the average density of w, T, C (in units of g/cm^3) within the tumor, and the radius growth during 180 days. The last three figures describe the densities of w, T, C along the radius of the tumor at day $t = 180$

the first simulation of the bottom row of Fig. 3, are also shrinking fast, for the same reason, in fact they recede so fast that the nearby reentrant corner is even decreasing.

5 Radially symmetric tumors: existence of solutions

In this section we prove existence and uniqueness of global in-time solutions in the case of radially symmetric tumors. Recall that the tumor boundary $r = R(t)$ satisfies the equation

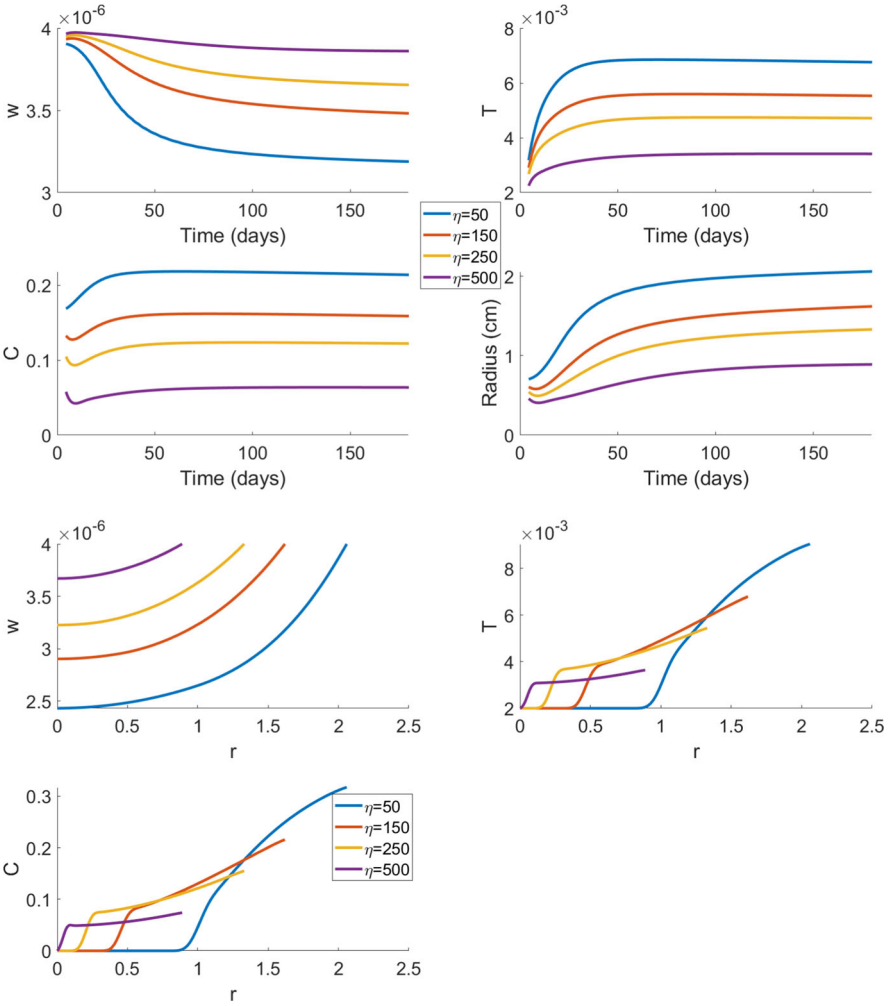

Fig. 2 Treatment with VEGF inhibitor, immune checkpoint blockade, and cancer vaccine. $W = w_0$ on the free boundary, with $\lambda_T = 4 \times 10^{-3}$ and $\varepsilon = 2$. The first four figures describe the dynamic of the average density of w, T, C (in units of g/cm^3) within the tumor, and the radius growth during 180 days. The last three figures describe the densities of w, T, C along the radius of the tumor at day $t = 180$

$$\frac{dR(t)}{dt} = \frac{3\mu(t)}{R(t)^2} \int_0^{R(t)} \left[\lambda_C \frac{[w - w_h]^+}{w_0 - w_h} C \left(1 - \frac{C}{K}\right) - \eta T C \right] r^2 \, dr. \tag{5.1}$$

We set

$$\begin{aligned} F_1(C, T, w) &= \lambda_C \frac{[w - w_h]^+}{w_0 - w_h} C\left(1 - \frac{C}{K}\right) - \eta T C, \\ F_2(C, T) &= \lambda_T C - \alpha_T (T - \varepsilon T_0), \\ F_3(C, w) &= -d_{wC} C w - d_w w, \end{aligned}$$

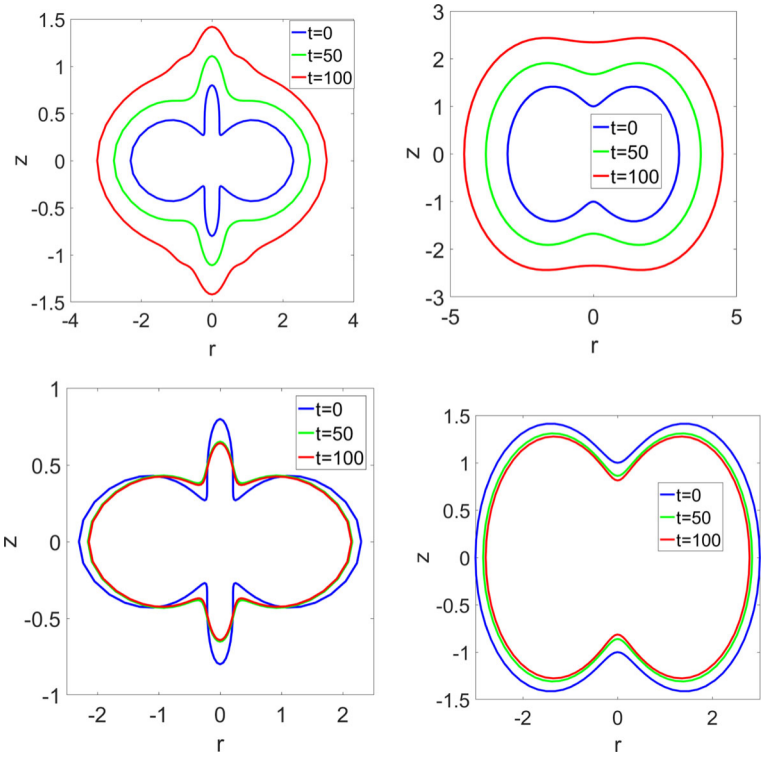

Fig. 3 Axially symmetric 3-D tumors with $W = w_0$ and $\lambda_T = 4 \times 10^{-3}$. The top row with $\eta = 1000$, $\varepsilon = 0$, the bottom row with $\eta = 10000$, $\varepsilon = 0.9$. Tumor volumes increase in the top row, and decrease in the bottom row

and rewrite the system (2.3, 2.7) in the form

$$\frac{\partial C}{\partial t} - \delta_C \frac{1}{r^2}\frac{\partial}{\partial r} r^2 \frac{\partial C}{\partial r} = F_1(C, T, w)\,\partial t \qquad \text{in } (t),\ t > 0, \tag{5.2}$$

$$\frac{\partial T}{\partial t} - \delta_T \frac{1}{r^2}\frac{\partial}{\partial r} r^2 \frac{\partial T}{\partial r} = F_2(C, T) \qquad \text{in } (t),\ t > 0, \tag{5.3}$$

$$\frac{\partial w}{\partial t} - \delta_w \frac{1}{r^2}\frac{\partial}{\partial r} r^2 \frac{\partial w}{\partial r} = F_3(C, w) \qquad \text{in } (t),\ t > 0, \tag{5.4}$$

with boundary conditions

$$\frac{\partial C}{\partial r}(R(t), t) = 0 \qquad \text{for } t > 0, \tag{5.5}$$

$$\frac{\partial T}{\partial r}(R(t), t) = \gamma(t)\,[T_0 - T(R(t), t)] \qquad \text{for } t > 0, \tag{5.6}$$

$$w(R(t), t) = W \qquad \text{for } t > 0. \tag{5.7}$$

We take initial conditions

$$C(r,0) = C_{in}(r), \quad T(r,0) = T_{in}(r), \quad w(r,0) = w_{in}(r) \quad \text{for } 0 \le r \le R(0). \tag{5.8}$$

We assume that C_{in}, T_{in}, w_{in} belong to $C^{2+\alpha}[0, R(0)]$ for some $0 \le \alpha < 1$, and satisfy

$$0 \le C_{in} \le K, \quad 0 \le T_{in} \le T_0, \quad 0 \le w_{in} \le W, \tag{5.9}$$

$$\frac{\partial C_{in}}{\partial r}(R(0)) = 0, \ w_{in}(R(0)) = W, \text{ and } \mu(t), \gamma(t) \text{ are in } C^{1+\alpha/2}[0,\infty),$$

$$\gamma(t) \text{ decreasing function, } \gamma(t) = 0 \text{ if } T \ge T_0 \text{ and } \gamma(t) > 0 \text{ if } T < T_0. \tag{5.10}$$

Theorem 5.1 *The system (5.1 – 5.10) has a unique solution for all $t > 0$, with $\frac{dR}{dt}$ in $C^{1+\alpha/2}[0,\infty)$ and C, T, w in $C^{2+\alpha,1+\alpha/2}(\Omega^\infty)$, where*

$$\Omega^\infty = \{(r,t) : 0 \le r \le R(t), 0 \le t < \infty\}.$$

We need the following lemma.

Lemma 5.2 *The following estimates hold for any solution of the system (5.1 – 5.10):*

$$0 \le w(r,t) \le W, \quad 0 \le C(r,t) \le K \quad \text{for } 0 \le r \le R(t), \ t > 0,$$

and

$$0 \le T(r,t) \le T_{max} \quad \text{for } 0 \le r \le R(t), \ t > 0,$$

where $T_{max} := \max\left\{\frac{\lambda_T K - d_T(1-\varepsilon)T_0}{d_T}, T_0\right\}$.

The first two estimates follow directly by comparing w (respectively C) with the constants W (respectively K) by the maximum principle, and the last bound on T follows by noting that T_{max} is a supersolution for T.

Proof of Theorem 5.1 We follow the proof of Theorem 2 in Friedmen et al. (2014), and begin with a change of variables

$$y = \frac{r}{R(t)}, \quad \hat{u}(y,t) = u(r,t) \quad \text{for } u = C, T, w,$$

in order to convert the system (5.1 – 5.10) with free boundary $r = R(t)$ to a system with a fixed boundary $y = 1$:

$$\frac{\partial \hat{C}}{\partial t} - \delta_C \frac{1}{y^2 R^2}\frac{\partial}{\partial y}\left(y^2 \frac{\partial \hat{C}}{\partial y}\right) - \frac{y\dot{R}}{R}\frac{\partial \hat{C}}{\partial y} = F_1(\hat{C}, \hat{T}, \hat{w}), \tag{5.11}$$

$$\frac{\partial \hat{T}}{\partial t} - \delta_T \frac{1}{y^2 R^2} \frac{\partial}{\partial y}\left(y^2 \frac{\partial \hat{T}}{\partial y}\right) - \frac{yR}{R}\frac{\partial \hat{T}}{\partial y} = F_2(\hat{C}, \hat{T}), \tag{5.12}$$

$$\frac{\partial \hat{w}}{\partial t} - \delta_w \frac{1}{y^2 R^2} \frac{\partial}{\partial y}\left(y^2 \frac{\partial \hat{w}}{\partial y}\right) - \frac{yR}{R}\frac{\partial \hat{w}}{\partial y} = F_3(\hat{C}, \hat{w}), \tag{5.13}$$

for $0 \le y \le 1$, $t > 0$,

$$\frac{\partial \hat{C}}{\partial y}(1, t) = 0, \tag{5.14}$$

$$\frac{1}{R}\frac{\partial \hat{T}}{\partial y}(1, t) = \gamma(t)[T_0 - \hat{T}(1, t)]^+, \tag{5.15}$$

$$\hat{w}(1, t) = W, \tag{5.16}$$

for $t > 0$, and

$$\frac{dR}{dt}(t) = 3\mu(t)R(t)\int_0^1 F_1(\hat{C}(y, t), \hat{T}(y, t), \hat{w}(y, t))y^2\, dy. \tag{5.17}$$

By Lemma 5.2,

$$0 \le \hat{C}(y, t) \le K, \quad 0 \le \hat{T}(y, t) \le T_{max}, \quad 0 \le \hat{w}(y, t) \le W,$$

and

$$|F_1(\hat{C}(y, t), \hat{T}(y, t), \hat{w}(y, t))| \le \frac{\lambda_C (W - w_h)}{w_0 - w_h} K + \eta T_{max} K \equiv F_{max}. \tag{5.18}$$

For any $0 < \tau < 1$, we define a mapping $R(t) \to \tilde{R}(t)$ from $C^{\alpha/2}[0, \tau]$ to $C^{\alpha/2}[0, \tau]$ as follows: Given $R(t)$, we solve the system for $\hat{C}$, $\hat{T}$, $\hat{w}$ and take

$$\frac{d}{dt}\tilde{R}(t) = 3\mu(t)\tilde{R}(t)\int_0^1 F_1(\hat{C}, \hat{T}, \hat{w})y^2\, dy, \qquad \tilde{R}(0) = R(0).$$

By (5.18),

$$\frac{d\tilde{R}}{dt}(t) \le \mu_\tau F_{max} R(t) \qquad \text{for } 0 \le t \le \tau, \tag{5.19}$$

where $\mu_\tau = \sup_{0 \le t \le \tau} \mu(t)$, and

$$R(0)e^{-\mu_\tau F_{max} t} \le \tilde{R}(t) \le R(0)e^{\mu_\tau F_{max} t}. \tag{5.20}$$

By Schauder estimates,

$$\|(\hat{C}, \hat{T}, \hat{w})\|_{C^{2+\alpha,1+\alpha/2}([0,1]\times[0,\tau])} \le M, \tag{5.21}$$

where M depends only on the parameters of the system.

We introduce the subset in $C^{\alpha/2}[0,\tau]$,

$$X = \{R \in C^{\alpha/2}[0,\tau] : R(0)e^{-\mu_\tau F_{max} t} \le R(t) \le R(0)e^{\mu_\tau F_{max} t},$$

and define the mapping $\Gamma_\tau : X \to X$ by $R \to \tilde{R}$. In view of (5.19) and (5.20), Γ_τ is a compact mapping from X into X.

We claim that Γ_τ is a contraction mapping if τ is small. To prove it we take any two functions R_1 and R_2 in X and their corresponding solutions $(C_i, T_i, \hat{w}_i)$ and $\tilde{R}_i = \Gamma_\tau(R_i)$, and consider the differences $\bar{C} = C_1 - C_2$, $\bar{T} = T_1 - T_2$, $\bar{w} = \hat{w}_1 - \hat{w}_2$, and the corresponding $\bar{R} = R_1 - R_2$. Then

$$\begin{aligned}
&\frac{\partial \bar{C}}{\partial t} - \delta_C \frac{1}{R_1^2 y^2}\frac{\partial}{\partial y} y^2 \frac{\partial \bar{C}}{\partial y} - \frac{1}{R_1} y\dot{\bar{R}}\frac{\partial C_1}{\partial y} = \bar{F}_1(y,t),\\
&\frac{\partial \bar{T}}{\partial t} - \delta_T \frac{1}{R_1^2 y^2}\frac{\partial}{\partial y} y^2 \frac{\partial \bar{T}}{\partial y} - \frac{yR_1}{R_1}\frac{\partial \bar{T}}{\partial y} = \bar{F}_2(y,t),\\
&\frac{\partial \bar{w}}{\partial t} - \delta_w \frac{1}{R_1^2 y^2}\frac{\partial}{\partial y} y^2 \frac{\partial \bar{w}}{\partial y} - \frac{y\dot{R}_1}{R_1}\frac{\partial \bar{w}}{\partial y} = \bar{F}_3(y,t),
\end{aligned}$$

where, as can be directly verified,

$$|\bar{F}_i(y,t)| \le A(|\bar{C}(y,t)| + |\bar{T}(y,t)| + |\bar{w}(y,t)| + |R_1(t) - R_2(t)|)$$

for some constant A. The $C^{\alpha,\alpha/2}$ norm of $\bar{F}_i$ can be estimated in a similar way. Then, by the Schauder estimates,

$$\|(\bar{C}, \bar{T}, \bar{w})\|_{C^{2+\alpha,1+\alpha/2}([0,1]\times[0,\tau])} \le A\|R_1 - R_2\|_{C^{\alpha/2}[0,\tau]}$$

and

$$\frac{d}{dt}(\log \tilde{R}_1 - \log \tilde{R}_2)(t) \le A\|R_1 - R_2\|_{C^{\alpha/2}[0,\tau]},$$

with another constant A.

Since $\tilde{R}_1(0) = \tilde{R}_2(0)$, we easily deduce that

$$[\tilde{R}_1 - \tilde{R}_2]_{C^{\alpha/2}[0,\tau]} \le \tau^{1-\alpha/2} A\|R_1 - R_2\|_{C^{\alpha/2}[0,\tau]}$$

and

$$\|\tilde{R}_1 - \tilde{R}_2\|_{C^0[0,\tau]} \le A\tau\|R_1 - R_2\|_{C^{\alpha/2}[0,\tau]}.$$

Taking τ sufficiently small we conclude that the mapping $_\tau$ is a contraction mapping, hence it has a unique fixed point. This completes the proof of existence and uniqueness in a small time interval $0 \le t \le \tau$.

The global existence follows from the a *priori* estimates

$$\frac{dR}{dt}(t) \le \mu_\tau F_{max} R(t)$$

and

$$R(0)e^{-\mu_\tau F_{max} t} \le R(t) \le R(0)e^{\mu_\tau F_{max} t}.$$

6 General domains: local existence of solutions

In this section we consider general domains (t) with free boundary $\partial(t)$, and prove existence and uniqueness of solutions of the model equations, for some time interval $0 \le t \le \tau, \tau > 0$.

Equations (5.2 5.3 and 5.4) are replaced by the following equations

$$\frac{\partial C}{\partial t} - \delta_C \nabla^2 C = F_1(C, T, w) \quad \text{in } (t),\ t > 0, \tag{6.1}$$

$$\frac{\partial T}{\partial t} - \delta_T \nabla^2 T = F_2(C, T) \quad \text{in } (t),\ t > 0, \tag{6.2}$$

$$\frac{\partial w}{\partial t} - \delta_w \nabla^2 w = F_3(C, w) \quad \text{in } (t),\ t > 0, \tag{6.3}$$

with the same functions F_j as in Sect. 5. We take boundary conditions

$$\frac{\partial C}{\partial n} = 0, \quad \frac{\partial T}{\partial n} + \gamma(t)(T - T_0) = 0, \quad w = W \quad \text{on } \partial(t),\ t > 0, \tag{6.4}$$

with a decreasing function $\gamma(t)$, $\gamma(t) = 0$ if $T \ge T_0$, $\gamma(t) > 0$ if $T < T_0$, and initial values

$$C(x, 0) = C_{in}(x), \quad T(x, 0) = T_{in}(x), \quad w(x, 0) = w_{in}(x) \quad \text{for } x \in (0). \tag{6.5}$$

We denote by $U(x, t)$ the velocity of cancer cells at the boundary, so that, by (2.8), the free boundary moves with velocity

$$U(x, t) = \rho(t) \nabla w(x, t) \quad \text{for} \quad x \in \partial(t),\ t > 0,$$

where $\rho(t)$ is defined in (2.10). However, in order to prove existence of solutions, we need to modify the definition of the velocity function by approximating it by a

smoother function: We accordingly define the velocity of the free boundary by

$$U(x,t) = \rho(t) \int w(x,t) j_\nu(x-x)dx, \tag{6.6}$$

where $j_\nu(y)$ is C^∞ function, $j_\nu(y) > 0$ if $|y| < \nu$, $j_\nu(y) = 0$ if $|y| > \nu$, and $j_\nu(y)dy = 1$. Here ν is arbitrarily small but fixed.

We make the following regularity assumptions:

$$\mu(t) \text{ and } \gamma(t) \text{ belong to } C^{1+\alpha/2}[0,\infty); \tag{6.7}$$

$$\partial(0) \in C^{3+\alpha}, \tag{6.8}$$

$$\begin{aligned} &\text{the functions } C_{in},\ T_{in},\ w_{in} \text{ are in } C^{2+\alpha}(\overline{(0)}), \text{ and have} \\ &C^{2+\alpha,1+\alpha} \text{ extensions to } \varepsilon_1 - \text{neighborhood of } \overline{(0)\times(0,\varepsilon_2)}, \text{ for} \\ &\text{some } \varepsilon_1, \varepsilon_2 > 0, \text{ for which the boundary conditions } (6.4) \text{ are} \\ &\text{satisfied at } \partial(0). \end{aligned} \tag{6.9}$$

Assuming the initial free boundary to be star-shaped, we expect it to remain star-shaped for a small time. We can then express the free boundary in the spherical coordinates:

$$\partial(t) = \{x \in \mathbb{R}^3 : x = Z(\lambda,t)\}, \tag{6.10}$$

where $\lambda = (\vartheta,\phi) \in := -_2, \underline{\pi} \times [0,2\pi]$, and

$$Z^0(\lambda) \equiv Z(\lambda,0) \in C^{3+\alpha}().$$

We denote by $e_r(\lambda)$, $e_\vartheta(\lambda)$, $e_\phi(\lambda)$ the local orthogonal unit vectors on the boundary $x = Z(\lambda,0)$ in the direction of increasing r, ϑ, ϕ, respectively, and write the surface $x = Z(\lambda,t)$ in the form

$$x = Z(\lambda,t) = Z^0(\lambda) + h(\lambda,t)e_r(\lambda). \tag{6.11}$$

Theorem 6.1 *The system (6.1) – (6.9) has a unique solution for some time interval $0 \le t \le \tau$ ($\tau > 0$) with free boundary of the form (6.11), such that*

$$\sup_{0\le t\le\tau} h(\cdot,t)_{C^{2+\alpha}()} + h_t(\cdot,t)_{C^{1+\alpha}()} < \infty. \tag{6.12}$$

Proof The proof uses similar arguments to those used in Friedman et al. (2012) in a model of wound healing. We first note that

$$\begin{aligned} &Z_t(\lambda,t) = h_t(\lambda,t)e_r(\lambda), \\ &Z_\vartheta(\lambda,t) = Z^0_\vartheta(\lambda) + h_\vartheta(\lambda,t)e_r(\lambda) + h(\lambda,t)e_\vartheta(\lambda), \\ &Z_\phi(\lambda,t) = Z^0_\phi(\lambda) + h_\phi(\lambda,t)e_r(\lambda) + h(\lambda,t)e_\phi(\lambda)\cos\vartheta. \end{aligned} \tag{6.13}$$

Taking scalar product with $e_r(\lambda)$, we get

$$h_t(\lambda, t) = Z_t(\lambda, t)e_r(\lambda), \tag{6.14}$$

$$h_\vartheta(\lambda, t) = Z_\vartheta(\lambda, t)e_r(\lambda) - Z^0_\vartheta(\lambda)e_r(\lambda), \tag{6.15}$$

$$h_\phi(\lambda, t) = Z_\phi(\lambda, t)e_r(\lambda) - Z^0_\phi(\lambda)e_r(\lambda). \tag{6.16}$$

As in Friedman et al. (2012), we shall express the velocity of the free boundary by a first order hyperbolic equation for $h(\lambda, t)$. To do that, consider the movement of a point $Z(\lambda, t + \Delta t)$ with $\lambda = (\vartheta, \phi)$ to a point $Z(\lambda + \Delta\lambda, t + \Delta t)$ with $\lambda = (\vartheta, \phi)$ at the time $t + \Delta t$, and set $\lambda = (\vartheta, \phi)$. We can write

$$Z(\lambda, t + \Delta t) - Z(\lambda, t) = [Z(\lambda, t + \Delta t) - Z(\lambda, t)] - [Z(\lambda, t) - Z(\lambda, t)] - [Z(\lambda, t) - Z(\lambda, t)],$$

and note that

$$\lim_{\Delta t\to 0} \frac{Z(\lambda, t + \Delta t) - Z(\lambda, t)}{\Delta t} = U(Z(\lambda, t), t) \cdot e_r,$$

$$\lim_{\Delta t\to 0} \frac{Z(\lambda, t) - Z(\lambda, t)}{\Delta t} = \lim_{\Delta t\to 0} \frac{Z(\lambda, t) - Z(\lambda, t)}{\vartheta - \vartheta} \cdot \lim_{\Delta t\to 0} \frac{\vartheta - \vartheta}{\Delta t}$$
$$= Z_\vartheta(\lambda, t)\frac{U(Z(\lambda, t), t) \cdot e_\vartheta}{|Z(\lambda, t)|},$$

$$\lim_{\Delta t\to 0} \frac{Z(\lambda, t) - Z(\lambda, t)}{\Delta t} = \lim_{\Delta t\to 0} \frac{Z(\lambda, t) - Z(\lambda, t)}{\phi - \phi} \cdot \lim_{\Delta t\to 0} \frac{\phi - \phi}{\Delta t}$$
$$= Z_\phi(\lambda, t)\frac{U(Z(\lambda, t), t) \cdot e_\phi}{|Z(\lambda, t)| \cos\vartheta}.$$

Hence

$$Z_t(\lambda, t) = U(Z(\lambda, t), t)e_r - Z_\vartheta(\lambda, t)\frac{U(Z(\lambda, t), t)) \cdot e_\vartheta}{|Z(\lambda, t)|} - Z_\phi(\lambda, t)\frac{U(Z(\lambda, t), t) \cdot e_\phi}{|Z(\lambda, t)| \cos\vartheta}.$$

Taking scalar product with e_r and using Eqs. (6.14–6.16), we obtain a hyperbolic differential equation for h:

$$h_t(\lambda, t) + \frac{U(Z(\lambda, t), t)) \cdot e_\vartheta}{|Z(\lambda, t)|} h_\vartheta(\lambda, t) + \frac{U(Z(\lambda, t), t)) \cdot e_\phi}{|Z(\lambda, t)| \cos\vartheta} h_\phi(\lambda, t) = G(\lambda, t), \tag{6.17}$$

where

$$G(\lambda, t) = U(Z(\lambda, t), t) \cdot e_r - Z^0_\vartheta(\lambda) \cdot e_r \frac{U(Z(\lambda, t), t \cdot e_\vartheta}{|Z(\lambda, t)|}$$
$$- Z^0_\phi(\lambda) \cdot e_r \frac{U(Z(\lambda, t), t)) \cdot e_\phi}{|Z(\lambda, t)| \cos\vartheta}, \tag{6.18}$$

and

$$h(\lambda, 0) = 0. \tag{6.19}$$

To prove Theorem 6.1 we shall use a fixed point argument in a closed subset of a Banach space,

$$X_{\tau M} = \{h(\lambda, t) : h(\lambda, 0) = 0, \quad h_\tau \le M\}, M > 0,$$

where

$$h_\tau = \sup_{0\le t\le\tau} h(\cdot, t)_{C^{2+\alpha}(\Omega)} + \sup_{0\le t\le\tau} h_t(\cdot, t)_{C^{1+\alpha}(\Omega)}.$$

From (6.6 and 6.11) we can compute $h_t(\lambda, 0)$, and note that $h_\tau \le \infty$ if $\tau = 0$; we choose M to be any number strictly greater than h_0. Given $h \in X_{\tau M}$, we define surfaces $x = Z(\lambda, t)$ by (6.11) and, using $C^{2+\alpha, 1+\alpha/2}$ Schauder estimate, solve the system (6.1–6.5), (6.7– 6.10). We use this solution to define a function $U(Z(\lambda, t), t)$ by (6.6), where $\rho(t)$ is defined by (2.10). We then introduce a function $\tilde{h}(\lambda, t)$ as the solution of the equation

$$\tilde{h}_t(\lambda, t) + \frac{U(Z(\lambda, t), t) \cdot e_\vartheta}{|Z_\lambda(\lambda, t)|}\tilde{h}_\vartheta(\lambda, t) + \frac{U(Z(\lambda, t), t) \cdot e_\phi}{|Z_\lambda(\lambda, t)| \cos\vartheta}\tilde{h}_\phi = G(\lambda, t), \tag{6.20}$$

with $\tilde{h}(\lambda, 0) = 0$.

We define a mapping A by $Ah = \tilde{h}$ and claim that if τ is small enough then A is a contraction mapping in $X_{\tau M}$; hence it has a unique fixed point, which is the unique solution asserted in Theorem 6.1.

To prove the claim we view (6.20) as an hyperbolic equation of the form

$$u_t + a(\lambda, t) \cdot \nabla_\lambda u = b(\lambda, t) \quad \text{for } \lambda \in \Omega, \ 0 \le t \le \tau, \tag{6.21}$$

with $u(\lambda, 0) = 0$, and

$$a(\cdot, t)_{C^{2+\alpha}(\Omega)} + b(\cdot, t)_{C^{2+\alpha}(\Omega)} \le B, \qquad \text{for } 0 \le t \le \tau.$$

From the proof of (Chen and Friedman 2003, Lemma 2.2) or (Friedman 2008, Lemma 3.2) we conclude that there exists a unique solution u of (6.21) with $u(\lambda, 0) = 0$, satisfying the estimate

$$u(\cdot, t)_{C^{2+\alpha}(\Omega)} \le C_0(B)\tau, \tag{6.22}$$

where the constant $C_0(B)$ depends only on B.

We denote by Ω_t the domain bounded by the surface defined by $h(\lambda, t)$, and by Ω_τ the 3-d domain spanned by Ω_t, $0 \le t \le \tau$. Since the lateral boundary of Ω_τ has

the same regularity as $h(\lambda, t)$, the $C^{2+\alpha, 1+\alpha/2}$ estimate on the solution of (6.1–6.5), (6.7– 6.10) imply, in particular, that

$$\sup_{0\le t\le\tau} U(Z(\cdot,t),t)\ {}^{2+\alpha}_{C}{}_{()}\ ,\le C_1(M),$$

where here, and in the sequel, $C_i(M)$ denote constants depending only on M.

We can therefore apply estimate (6.22) to the solution $\tilde{h}(\lambda, t)$ of (6.20) (with $\tilde{h}(\lambda, 0) = 0$) and conclude that

$$h(\tilde{\cdot}, t)_{C^{2+\alpha}()} \le C_2(M)\tau.$$

From (6.20) it then follows that

$$h_{\tilde{t}}(\cdot, t)_{C^{2+\alpha}()} \le C_3(M)\tau.$$

Taking τ such that $[C_2(M) + C_3(M)]\tau < M$, we deduce that $A : h \to \tilde{h}$ maps $X_{\tau M}$ into itself.

To prove that A is a contraction, we take h_1, h_2 in $X_{\tau M}$ with the corresponding $Z_i(\lambda, t)$, the solutions (C_i, T_i, w_i) and $U_i(Z_i(\lambda, t), t)$, $G_i(\lambda, t)$, and domains $(\Gamma_{\tau,i}$ $i = 1, 2)$, and set

$$\delta = (h_1 - h_2)_\tau.$$

We transform $\Gamma_{t,2}$ into $\Gamma_{t,1}$ by change of variables

$$\tilde{r} = r - (h_2 - h_1)(\lambda, t)\cdot\psi,$$

where ψ is a C^3 function with compact support that is equal to 1 in a neighborhood of the initial domain. The functions C_2, T_2, w_2 in the original variables (r, λ) in $\Gamma_{t,2}$ become functions $\tilde{C}_2$, $\tilde{T}_2$, $\tilde{w}_2$ in the variables $(\tilde{r}, \lambda)$ in $\Gamma_{t,1}$ and they satisfy a similar system of equations and boundary conditions as C_1, T_1, w_1, but with somewhat different coefficients, in such a case, we have

$$C_1 - \tilde{C_2}, T_1 - \tilde{T_2}, w_1 - \tilde{w}_{2C^{\alpha,\alpha/2}(\Gamma_{\tau,1})} \le C_4(M)(h_1 - h_2)(\cdot, t)_{C^{2+\alpha}()} \le C_4(M)\delta.$$

Using the Schauder estimates, we get

$$C_1 - \tilde{C_2}, T_1 - \tilde{T_2}, w_1 - \tilde{w}_{2C^{2+\alpha,1+\alpha/2}(\Gamma_{\tau,1})} \le C_5(M)\delta. \tag{6.23}$$

We can then extend the solutions (C_i, T_i, w_i) to $\bar{\Gamma}_{\tau,1}$ so that the estimate (6.23) yields the estimate

$$C_1 - C_2, T_1 - T_2, w_1 - w_{2C^{2+\alpha,1+\alpha/2}(\Gamma_{\tau,2})} \le C_6(M)\delta. \tag{6.24}$$

As before, the same estimate holds also for the λ-derivative of the differences, so that

$$(U_1 - U_2)(\cdot, t), (G_1 - G_2)(\cdot, t)_{C^{2+\alpha}()} \le C_7(M)\delta. \tag{6.25}$$

We now write the equations for $\tilde{h}_1$ and $\tilde{h}_2$ in integrated form along their respective characteristics, and note that, by (6.25), the characteristic curves are close to each other in the $C^{2+\alpha}$-norm. Proceeding as in (Chen and Friedman 2003; Friedman 2008), we can then successively estimate $\tilde{h}_1 - \tilde{h}_2$, $\partial_\lambda(\tilde{h}_1 - \tilde{h}_2)$, $\partial_\lambda^2(\tilde{h}_1 - \tilde{h}_2)$ in their $C^\alpha()$ norm, for any fixed t, and thus derive the estimate

$$(\tilde{h_1} - \tilde{h_2})(\cdot, t)_{C^{2+\alpha}()} \le C_8(M)\delta\tau.$$

From the differential equations for $\tilde{h_1}, \tilde{h_2}$ we then also derive the estimate

$$\frac{\partial}{\partial t}(\tilde{h_1} - \tilde{h_2})(\cdot, t) \quad \le C_9(M)\delta\tau. \; C^{1+\alpha}()$$

Hence, if τ is sufficiently small then

$$\tilde{h_1} - \tilde{h_{2\tau}} \le \frac{\delta}{2} h_1 - h_{2\tau},$$

so that the mapping A is a contraction, and the unique fixed point of A then provides the unique solution asserted in Theorem 6.1.

7 Analysis of the radially symmetric case

Lemma 7.1 *If* $\varepsilon > 0$, *and*

$$\varepsilon T_0 \le T_{i\,n}(r) \le T_{max} \quad \text{and} \quad 0 < C_{in}(r) \le C_{max} := K1 - \frac{T_0}{\lambda \frac{\eta\varepsilon}{C} W_0 - \frac{h}{w}}$$

in $[0, R_{in}]$, *then we have the following:*

$$\varepsilon T_0 \le T(r, t) \le T_{max}, \qquad \inf_{[0, R_{in}]} C_{in} \; e^{-\eta T^{max} t} \le C(r, t) \le C_{max} \tag{7.1}$$

for $0 \le r \le R(t)$, $t \ge 0$.

Proof It is easy to see that $\underline{T}(r, t) \equiv \varepsilon T_0$ is a sub-solution of the equation of T:

$$\begin{cases} \frac{\partial}{\partial t}\underline{T} - \delta_T \underline{T} \le \lambda_T C(r, t) - \alpha_T(\underline{T} - \varepsilon T_0) & \text{for } 0 \le r \le R(t),\ t > 0, \\ \frac{\partial}{\partial r}\underline{T}(R(t), t) = 0 \le \gamma(t)[T_0 - T(R(t), t)]^+ & \text{for } t > 0, \\ \underline{T}(r, 0) \le T_{in}(r) & \text{for } 0 \le r \le R_{in}. \end{cases}$$

By comparison, and recalling the upper bound from Lemma 5.2, we have $\varepsilon T_0 \le T \le T_{max}$. Next, we estimate C by observing that it satisfies the inequality

$$\frac{\partial}{\partial t} C - \delta_C C \le \lambda_C \cdot \frac{W - w_h}{w_0 - w_h} C \left(1 - \frac{T_0}{\lambda \frac{\eta \varepsilon}{C} \frac{W - w_h}{w_0 - w_h} K}\right) \frac{C}{}$$

with the Neumann boundary condition on $r = R(t)$. We again deduce by comparison the desired upper bound for C. Finally, the lower bound of C follows by observing that the function $C_\square(t) = e^{-\eta T_{max} t} \min_{[0, R(t)]} C(\cdot, 0)$ satisfies

$$\frac{d}{dt} C_\square(t) = -\eta T_{max} C_\square(t) \quad \text{for } t \ge 0,$$

and is a subsolution for $C(r, t)$.

Define $\sigma(r) = \frac{\sinh(r)}{r}$, and for $\tilde{R} > 0$, define

$$\underline{\sigma}(r; \tilde{R}) = \frac{}{\sigma \frac{W}{d_{wC} \frac{K + d_w \sigma}{\delta_w} \tilde{R}}} \sqrt{\frac{d_{wC} K + d_w}{\delta_w}} r \quad .$$

Lemma 7.2 *Suppose $w_{in} \ge \underline{\sigma}(r; R_{in})$ for $0 \le r \le R_{in}$, then*

$$w(r, t) \ge \underline{w}(r, t) := \underline{\sigma}(r; R_{max}(t)) \quad \text{for } 0 \le r \le R(t),\ t > 0,$$

where $R_{max}(t) := \max_{0 \le t \le t} R(t)$.

Proof Indeed, using the facts that $\frac{\partial}{\partial t} w(r, t) \le 0$ and $0 \le C(r, t) \le K$, we observe that $\underline{w}(r, t)$ satisfies

$$\begin{cases} \frac{\partial}{\partial t} \underline{w} - \delta_w \underline{w} \le -d_{wC} C \underline{w} - d_w \underline{w} & \text{for } 0 \le r \le R(t),\ t > 0, \\ \underline{w}(R(t), t) \le W & \text{for } t > 0, \\ \underline{w}(r, 0) \le w_{in}(r) & \text{for } 0 \le r \le R_{in}. \end{cases}$$

It follows by comparison that $w(r, t) \ge \underline{w}(r, t)$.

7.1 $R(t)$ is shrinking if is large

Theorem 7.3 *If $\varepsilon > 0$, $\varepsilon T_0 \le T_{in}(r) \le T_{max}$, and*

$$\eta > \frac{\lambda_C}{\varepsilon T_0} \cdot \frac{W - w_h}{w_0 - w_h},$$

then $\frac{d}{dt} R(t) < 0$ for all $t \ge 0$. In particular, $\lim_{t \to +\infty} R(t) \in [0, R_{in})$ exists.

Proof Indeed,

$$\frac{d}{dt}R(t) = \frac{3\mu(t)}{R(t)^2}\int_0^{R(t)} \lambda^C \frac{[w(r,t)-w_h]^+}{w_0-w_h} C\left(1-\frac{C}{K}\right) - \eta T C\, r^2\, dr$$
$$\le \frac{3\mu(t)}{R(t)^2} C\left(\lambda_C \frac{W-w_h}{w_0-w_h} - \eta(\varepsilon T_0)\right) r^2\, dr < 0,$$

for $t \ge 0$. Here we used the estimates $0 \le w(r,t) \le W$ (Lemma 5.2), and $T(r,t) \ge \varepsilon T_0$ (Lemma 7.1).

7.2 $R(t)$ is increasing for $0 \le$ 1

Lemma 7.4 *Given R_{in}, there exists $0 < \delta < \min\{1, 2R_{in}/3\}$ such that*

$$\inf_{r\in[\tilde{R}-\delta,\tilde{R}]} \sigma(r;\tilde{R}) \ge \frac{W+w_h}{2} \quad \text{for each } \tilde{R}\in[R_{in},\infty).$$

Proof Since $\sigma(\tilde{R};\tilde{R}) = W > \frac{W+w_h}{2}$, and

$$\sup_{\tilde{R}\in[R_{in},\infty)} \left\| \frac{\partial\sigma}{\partial r}(\cdot;\tilde{R}) \right\|_{L^\infty([0,\tilde{R}])} < +\infty,$$

the assertion follows for any sufficiently small $\delta > 0$.

Remark 7.5 Using the fact that $\delta \in (0, 2R_{in}/3)$, we have

$$\frac{\tilde{R}^3-(\tilde{R}-\delta)^3}{\tilde{R}^2} > 3\delta - \frac{3\delta^2}{\tilde{R}} \ge \delta, \quad \text{for } \tilde{R}\in[R_{in},\infty).$$

Lemma 7.6 *Given $R_{in} > 0$ and $\mu(t) > 0$ satisfying $\int_0^\infty \mu(t)\,dt = +\infty$, denote by $G_\eta(t)$, for any $\eta > 0$, the unique solution of*

$$\frac{d}{dt}G(t) = \eta(t, G(t)) \quad \text{for } t\in[0,\infty), \qquad \text{and} \quad G(0) = R_{in},$$

where

$$\eta(t,G) = \mu(t)\lambda_C \frac{W-w_h}{2(w_0-w_h)}\delta\frac{(1-C_{max}/K)}{\hat{R}} e^{-\eta T_{max} t} - \eta T_{max} C_{max} G. \quad (7.2)$$

Then for each $\hat{R}\in(R_{in},\infty)$, there exist $\hat{\eta}, \hat{t} > 0$ such that

$$\frac{d}{dt}G^{\hat{\eta}}(t) > 0 \quad \text{in } [0,\hat{t}], \quad \text{and} \quad G^{\hat{\eta}}(\hat{t}) = \hat{R}.$$

Proof Fix $R_{in} < \hat{R}$. When $\eta = 0$, we can make use of the condition $\int_0^\infty \mu(t)\,dt = \infty$ to deduce $G(t) \to \infty$ as $t \to \infty$. Hence, for arbitrarily large R, there exists $\hat{t}$ such that $G(t) > 0$ in $[0, \hat{t}]$ and $G(\hat{t}) = R + 1$. Since the solution depends continuously on the parameter η, there exists a small $\hat{\eta}$ such that for $\eta \in (0, \hat{\eta}]$, we have $G(t) > 0$ in $[0, \hat{t}]$ and $G(\hat{t}) > R$. The lemma holds by choosing $\hat{t}$ to be the unique point in $(0, \hat{t})$ such that $G(\hat{t}) = R$.

Theorem 7.7 *Let $\mu(t) > 0$ be given such that $\int_0^\infty \mu(t)\,dt = +\infty$, and, for any $R \geq R_{in}$, let $\hat{\eta}, \hat{t}$ be given by Lemma 7.6. Suppose*

$$\varepsilon T_0 \leq T_{in}(r) \leq T_{max}, \quad w_{in}(r) \geq \underline{\sigma}(r; R_{in}), \quad C_{in}(r) \geq \frac{1}{\hat{R}} \quad \text{in } [0, R_{in}].$$

Then, for any $\eta \in [0, \hat{\eta}]$, there exists $t_\eta \leq \hat{t}$ such that

$$\frac{d}{dt} R(t) > 0 \quad \text{in } [0, t_\eta], \quad \text{and} \quad R(t_\eta) = \hat{R}. \tag{7.3}$$

Proof Define the set

$$I := \{t \in [0, t_\eta] : \frac{d}{dt} R(t) > 0 \quad \text{in } [0, t]\}. \tag{7.4}$$

It is clear that I is connected and is open relative to $[0, t_\eta]$. Next, we show that $I \neq 0$. Indeed, by (5.1), we have

$$\begin{aligned}
\frac{d}{dt} R(0) &= \frac{3\mu(0)}{R_{in}^2} \int_0^{R_{in}} \lambda_C \frac{[w_{in} - w_h]^+}{w_0 - w_h} C\left(1 - \frac{C}{K}\right) - \eta T C \, r^2\,dr \\
&\geq \frac{3\mu(0)}{R_{in}^2} \int_0^{R_{in}} \lambda_C \frac{[\underline{\sigma}(r; R_{in}) - w_h]^+}{w_0 - w_h} C(r, 0)(1 - C_{max}/K) - \hat{\eta} T_{max} K \, r^2\,dr \\
&\geq \frac{3\mu(0)}{R_{in}^2} \int_{R_{in}-\delta}^{R_{in}} \lambda_C \frac{(W - w_h)/2}{w_0 - w_h} (1 - C_{max}/K)(\inf C_{in}) e^{-\hat{\eta} T_{max} \cdot 0} r^2\,dr \\
&\quad - \int_0^{R_{in}} \hat{\eta} T_{max} C_{max} r^2\,dr \\
&\geq \mu(0) \lambda_C \frac{(W - w_h)/2}{w_0 - w_h} \frac{(1 - C_{max}/K)}{\hat{R}} \delta - \hat{\eta} T_{max} C_{max} R_{in},
\end{aligned}$$

where we used $C \leq C_{max}$, $T \leq T_{max}$ (see 7.1) for the first inequality; $w_{in} \geq \underline{\sigma}(r; R_{in})$, and Lemma 7.4 for the second inequality, and Remark 7.5 in the last inequality. By comparison, we have $\frac{dR}{dt}(0) \geq \frac{dG}{dt}(0) > 0$, where G is given in Lemma 7.6. This proves that $I \neq 0$.

Since I is nonempty, $t^* := \sup I \in (0, t_\eta]$ and $\frac{dR}{dt} > 0$ in $[0, t^*)$. We claim that $R(t^*) \geq \hat{R}$. Suppose to the contrary, then that $R(t) < \hat{R}$ for $0 \leq t < t^*$. By Lemma 7.2, $w(r, t) \geq \underline{\sigma}(r; R(t))$ for $t \in [0, t^*]$. Hence, we can repeat the above argument to show

that for $t \in [0, t^*]$,

$$\frac{d}{dt} R(t) \geq \hat{\eta}(t, R(t)), \tag{7.5}$$

where $\hat{\eta}$ is given in (7.2). Since $R(0) = G^{\hat{\eta}}(0) = R_{in}$, we get, by comparison,

$$R_{in} \leq G^{\hat{\eta}}(t) \leq R(t) < \hat{R} \quad \text{for } t \in [0, t^*].$$

This immediately yields $t^* < \hat{t}$, since $G^{\hat{\eta}}(\hat{t}) \geq \hat{R}$. However, by Lemma 7.6, since $\hat{\mu}(t, R(t)) > 0$ as long as $R(t) \leq \hat{R}$, we deduce from (7.5) that $\frac{d}{dt} R(t) > 0$ in $[0, t^*]$, i.e., $[0, t^*] \subset I$. Since I is open, we have $\sup I > t^*$, and this contradicts the fact that $t^* = \sup I$. Having proved that $R(t^*) \geq \hat{R}$, we conclude that there exists a $t^* \in (0, \hat{t}]$ such that

$$\frac{d}{dt} R(t) > 0 \quad \text{in } [0, t^*] \quad \text{and} \quad R(t^*) \geq \hat{R}.$$

We can then choose $\hat{t}_\eta$ to be the unique number in $[0, t^*]$ such that $R(\hat{t}_\eta) = \hat{R}$, and this completes the proof.

Corollary 7.8 *If $\mu(t) \leq \mu_0(1 + t)$ for some $\mu_0 > 0$, then*

$$\hat{t}_\eta \geq \frac{2(w_0 - w_h)}{\mu_0 \lambda_C (W - w_h) K} \log \left(\frac{\hat{R}}{R_{in}} \right)^{1/2} - 1. \tag{7.6}$$

In particular, the interval where $R(t)$ is increasing initially can be made arbitrarily large by choosing $\hat{R}$ large.

Proof of Corollary 7.8 Let $\hat{t}_\eta > 0$ be given such that (7.3) holds. Using (5.1) and that $\mu(t) \leq \mu_0(1 + t)$, we have

$$\frac{d}{dt} \log R(t) \leq \mu_0(1 + t) \lambda_C \frac{W - w_h}{w_0 - w_h} \cdot K.$$

Integrating from 0 to $\hat{t}_\eta$, we obtain

$$\log \frac{\hat{R}}{R_{in}} \leq \frac{\mu_0 \lambda_C (W - w_h) K}{w_0 - w_h} \hat{t}_\eta + \frac{\hat{t}_\eta^2}{2} \leq \frac{\mu_0 \lambda_C (W - w_h) K}{w_0 - w_h} \frac{(1 + \hat{t}_\eta)^2}{2},$$

from which (7.6) follows.

8 Conclusion

Cancer cells within a tumor move toward sources of oxygen and nutrients; cells in the tumor core are mostly in the necrotic state. As a result, the density of cancer cells varies significantly within the tumor, and it increases toward the tumor boundary. In this paper, we developed a simple mathematical model that accounts for this density variability. The model includes, in addition to cancer cells, cytotoxic T cells, and oxygen. The model consists of three partial differential equations, and the tumor boundary is a free boundary. Some of the model parameters represent anti-cancer drugs. The dynamics of the free boundary is determined by the assumption that cancer cells at the boundary move in the direction of the oxygen gradient.

We simulated the model in cases of radially symmetric and axially symmetric tumors, and illustrated situations when the tumor volume grows when treated with "weak" drugs, and shrinks when treated with "strong" drugs. We next proved, by analysis, that the free boundary problem has a global solution in the radially symmetric case and local in-time solution for general shaped tumors. Finally, in the radially symmetric case, we proved under some (strong) assumptions, that the tumor radius may decrease monotonically or increase monotonically.

In this paper, we used oxygen as the driving force in tumor cell migration and proliferation. Another approach was proposed by Gatenby and Gawlinsti, based on the Warburg effect which asserts that malignant cells have increased reliance on aerobic metabolism of glucose to lactic acid (Gatenby and Gawlinski 1996, 2003). Based on tumor-induced acidification, they developed a mathematical model consisting of three reaction-diffusion equations, for tumor cells, healthy cells, and lactic acid, in a fixed domain. The model was extended in later studies to include, in particular, tumor growth in the form of a traveling wave, and travelling wave analysis (McGillen et al. 2014; Colson et al. 2021); see also references in (McGillen et al. 2014; Colson et al. 2021) on other extensions of the model.

Both oxygen and glucose contribute to the microenvironment of a tumor. It would be interesting, in future work, to include both oxygen and glucose, healthy cells and tumor cells, as well as T cells and other immune cells and cytokines that play a role in the interactions among these cells.

We finally note that our existence proof for the free boundary problem in the radially symmetric case follows the same technique as in the generic class of Stefan problems; however, in the case of general domains, the situation is quite different. Existence proofs for free boundary problems in general domains depend, in a very delicate way, on the specific dynamics of the free boundary.

Funding KYL is supported by NSF Grant DMS-1853561 and WH is supported by NSF Grant DMS-2052685.

References

Byrne HM, Chaplain MAJ (1997) Free boundary value problems associated with the growth and development of multicellular spheroids. Eur J Appl Math 8(6):639–658

Chen X, Friedman A (2003) A free boundary problem for an elliptic-hyperbolic system: an application to tumor growth. SIAM J Math Anal 35(4):974–986
Colson C, Sánchez-Garduño F, Byrne HM, Maini PK, Lorenzi T (2021) Travelling-wave analysis of a model of tumour invasion with degenerate, cross-dependent diffusion. Proc Math Phys Eng Sci 477(2256):20210593
Dini S, Binder BJ, Fischer SC, Mattheyer C, Schmitz A, Stelzer EHK, Bean NG, Green JEF (2016) Identifying the necrotic zone boundary in tumour spheroids with pair-correlation functions. J Royal Soc Interface 13(123):20160649
Fares CM, Van Allen EM, Drake CG, Allison JP, Hu-Lieskovan S (2019) Mechanisms of resistance to immune checkpoint blockade: why does checkpoint inhibitor immunotherapy not work for all patients? Am Soc Clin Oncol Educ Book 39:147–164
Freyer JP, Sutherland RM (1986) Proliferative and clonogenic heterogeneity of cells from EMT6/Ro multicellular spheroids induced by the glucose and oxygen supply. Cancer Res 46(7):3513–3520
Friedman A (2008) A multiscale tumor model. Interfaces Free Bound 10(2):245–262
Friedman A (2018) Mathematical biology, vol 127. American Mathematical Soc, US
Friedman A, Hao W (2015) A mathematical model of atherosclerosis with reverse cholesterol transport and associated risk factors. Bull Math Biol 77(5):758–781
Friedman A, Siewe N (2020) Mathematical model of chronic dermal wounds in diabetes and obesity. Bull Math Biol 82(10):1–33
Friedman A, Tian JP, Giulia Fulci E, Chiocca A, Wang J (2006) Glioma virotherapy: effects of innate immune suppression and increased viral replication capacity. Cancer Res 66(4):2314–2319
Friedman A, Bei H, Xue C (2012) A three dimensional model of wound healing: analysis and computation. Discrete Contin Dyn Syst Ser B 17(8):2691–2712
Friedmen A, Kao C-Y, Leander R (2014) On the dynamics of radially symmetric granulomas. J Math Anal Appl 412(2):776–791
Gallaher JA, Brown JS, Anderson ARA (2019) The impact of proliferation-migration tradeoffs on phenotypic evolution in cancer. Sci Rep 9(1):1–10
Gatenby RA, Gawlinski ET (1996) A reaction-diffusion model of cancer invasion. Cancer Res 56(24):5745–5753
Gatenby RA, Gawlinski ET (2003) The glycolytic phenotype in carcinogenesis and tumor invasion: insights through mathematical models. Cancer Res 63(14):3847–3854
Gupta R, Emens LA (2010) GM-CSF-secreting vaccines for solid tumors: moving forward. Discov Med 10(50):52
Hao W, Friedman A (2014) The LDL-HDL profile determines the risk of atherosclerosis: a mathematical model. PloS One 9(3):e90497
Hao W, Schlesinger LS, Friedman A (2016) Modeling granulomas in response to infection in the lung. PLoS One 11(3):e0148738
Kaufman HL, Ruby CE, Hughes T, Slingluff CL (2014) Current status of granulocyte-macrophage colony-stimulating factor in the immunotherapy of melanoma. J Immunother Cancer 2(1):1
Lai X, Friedman A (2019) How to schedule VEGF and PD-1 inhibitors in combination cancer therapy? BMC Syst Biol 13(1):30
Li X, Shao C, Shi Y, Han W (2018) Lessons learned from the blockade of immune checkpoints in cancer immunotherapy. J Hematol Oncol 11(1):1–26
McGillen JB, Gaffney EA, Martin NK, Maini PK (2014) A general reaction-diffusion model of acidity in cancer invasion. J Math Biol 68(5):1199–1224
Nicolae M, Avner F (2020) A mathematical model of the multiple sclerosis plaque. J Theor Biol 512:110532
Postow MA, Callahan MK, Wolchok JD (2015) Immune checkpoint blockade in cancer therapy. J Clin Oncol 33(17):1974
Salmond RJ (2018) mTOR regulation of glycolytic metabolism in T cells. Front Cell Dev Biol 6:122
Siewe N, Yakubu A-A, Satoskar AR, Friedman A (2017) Granuloma formation in leishmaniasis: a mathematical model. J Theor biol 412:48–60
Simmons AD, Li B, Gonzalez-Edick M, Lin C, Moskalenko M, Thomas D, Creson J, VanRoey MJ, Jooss K (2007) GM-CSF-secreting cancer immunotherapies: preclinical analysis of the mechanism of action. Cancer Immunol Immunother 56(10):1653–1665
van der Burg SH, Arens R, Ossendorp F, van Hall T, Melief CJM (2016) Vaccines for established cancer: overcoming the challenges posed by immune evasion. Nat Rev Cancer 16(4):219–233

van der Windt GJW, Pearce EL (2012) Metabolic switching and fuel choice during T-cell differentiation and memory development. Immunol Rev 249(1):27–42
Wu J, Waxman DJ (2018) Immunogenic chemotherapy: dose and schedule dependence and combination with immunotherapy. Cancer Lett 419:210–221, 04